GSA Data Repository Item 2015G37486

Did the AD 365 Crete earthquake/tsunami trigger synchronous giant turbidity currents in the Mediterranean Sea?

Polonia A., Vaiani S.C., and de Lange G., 2016.

Did the A.D. 365 Crete earthquake/tsunami trigger synchronous giant turbidity currents in the Mediterranean Sea?

***Geology*, March 2016, v. 44, p. 191-194, 2016, doi:10.1130/G37486.1**

DATA REPOSITORY

Data Repository DR1 - THE HOMOGENITE/AUGIAS TURBIDITE IN CORE CALA05

Core CALA05 (3800 m water depth), collected in an enclosed basin adjacent the abyssal plain at the base of the Malta escarpment (DR2), represents a key sample as it was used to define the Homogenite/Augias turbidite (HAT) composition and emplacement time in the Western Ionian Sea (Polonia et al., 2013a). In this core, the HAT is 1.84 m thick and is located stratigraphically between Sapropel S-1 and three terrigenous sandy/silty turbidites (T1, T2, T3) possibly triggered by the AD 1908, 1693 and 1169 earthquakes (Polonia et al., 2013b). The base of the megabed is defined by a sharp increase in sand content, containing a mixture of detrital (plagioclase, basaltic glass, carbonate grains, pyrite incrustations), and shelf/slope biogenic components. In contrast, the upper part of the turbidite consists of structureless mud. Sedimentological and geochemical analyses of the core point to a multisource turbidite deposit with different composition and provenance, which includes the Malta escarpment, Calabrian margin and Sicily channel.

Radiocarbon ages were obtained from planktonic foraminifera in pelagic sediments (P) above and beneath the HAT. Age modeling and correlation with results from adjoining cores showed a likely emplacement time of AD 215-530 (Polonia et al., 2013a). The recovery in the same core of both the HAT and the Santorini event (T6 turbidite) is a key element in support of a younger age of the HAT megaturbidite.

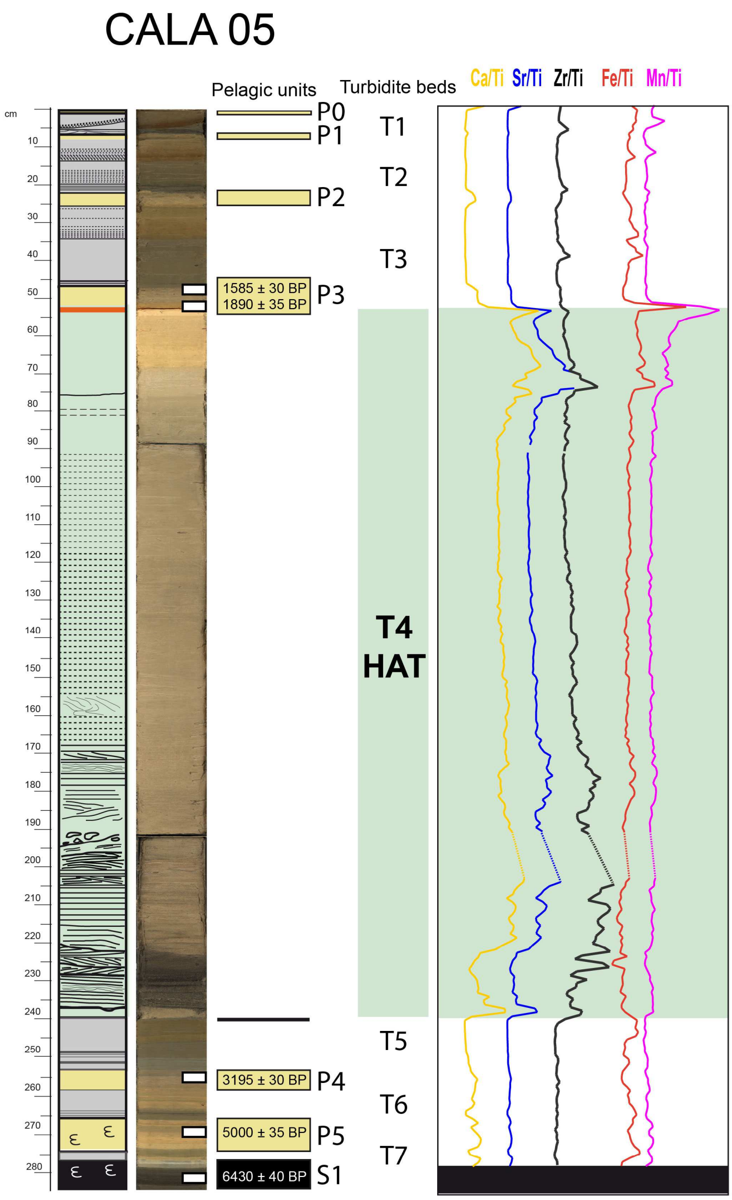

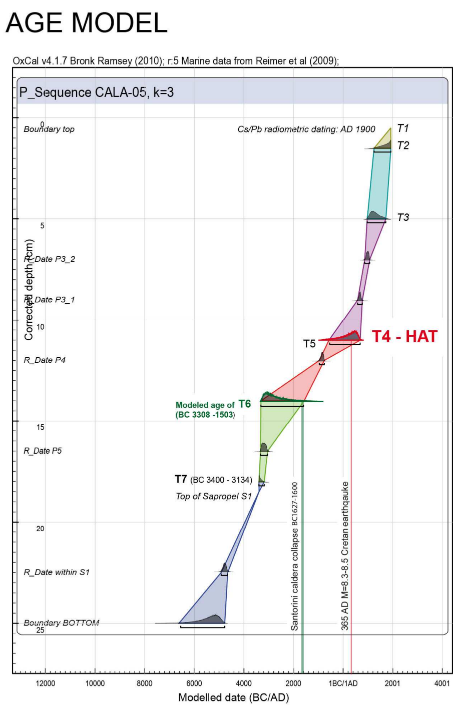

Data Repository DR 2

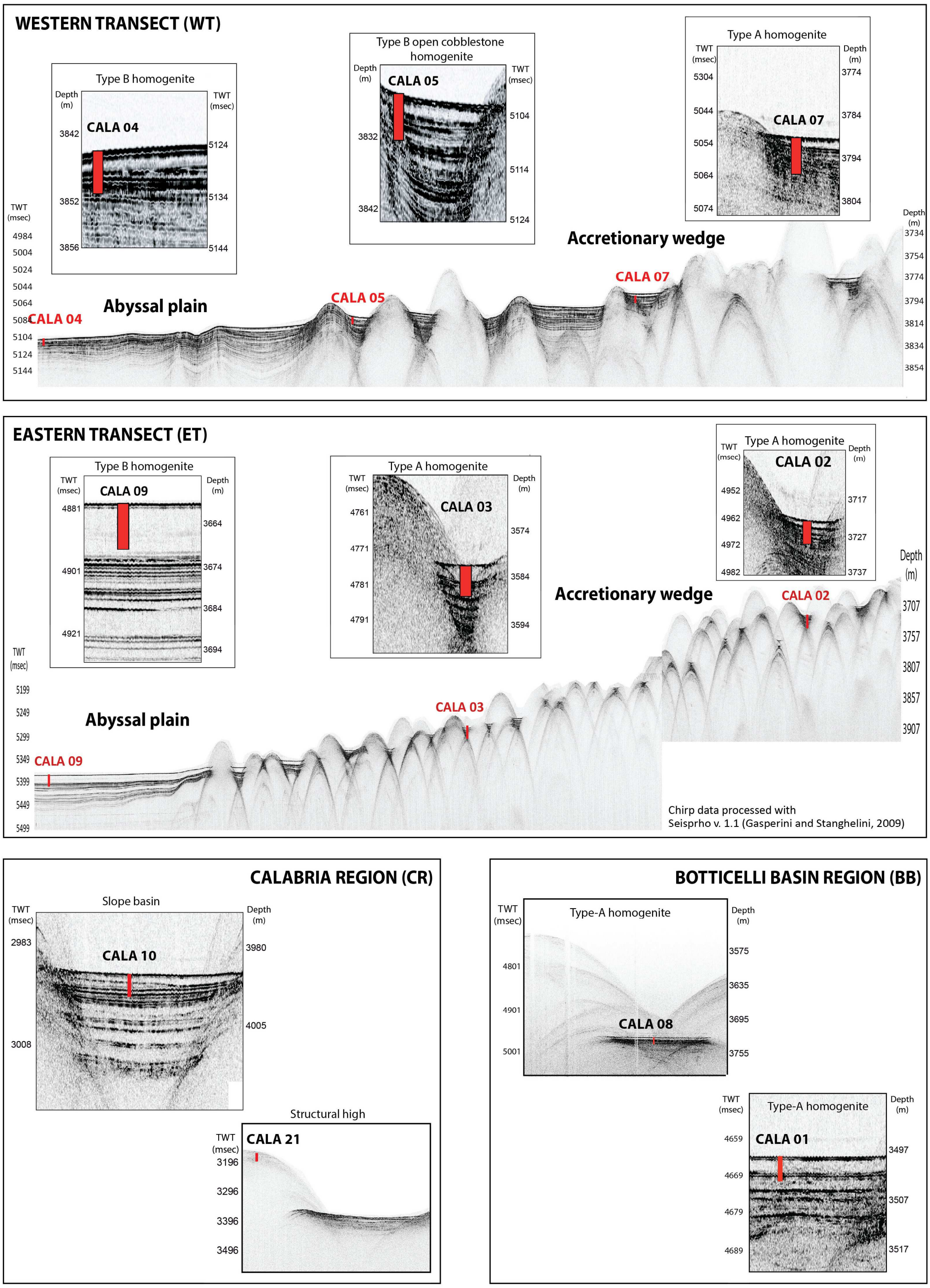

DR2: Sub-bottom CHIRP profiles across the coring sites investigated in this study (see Fig. 1 for location of Chirp profiles and gravity cores). The two long profiles across the Eastern and Western transects are collected at the transition between the undeformed abyssal plain and the accretionary wedge. Gravity cores are represented by red rectangles on the CHIRP profiles. Seismic data have been processed and geo-referenced using the open-source software Seisprho (Gasperini and Stanghellini, 2009).

Data repository DR3

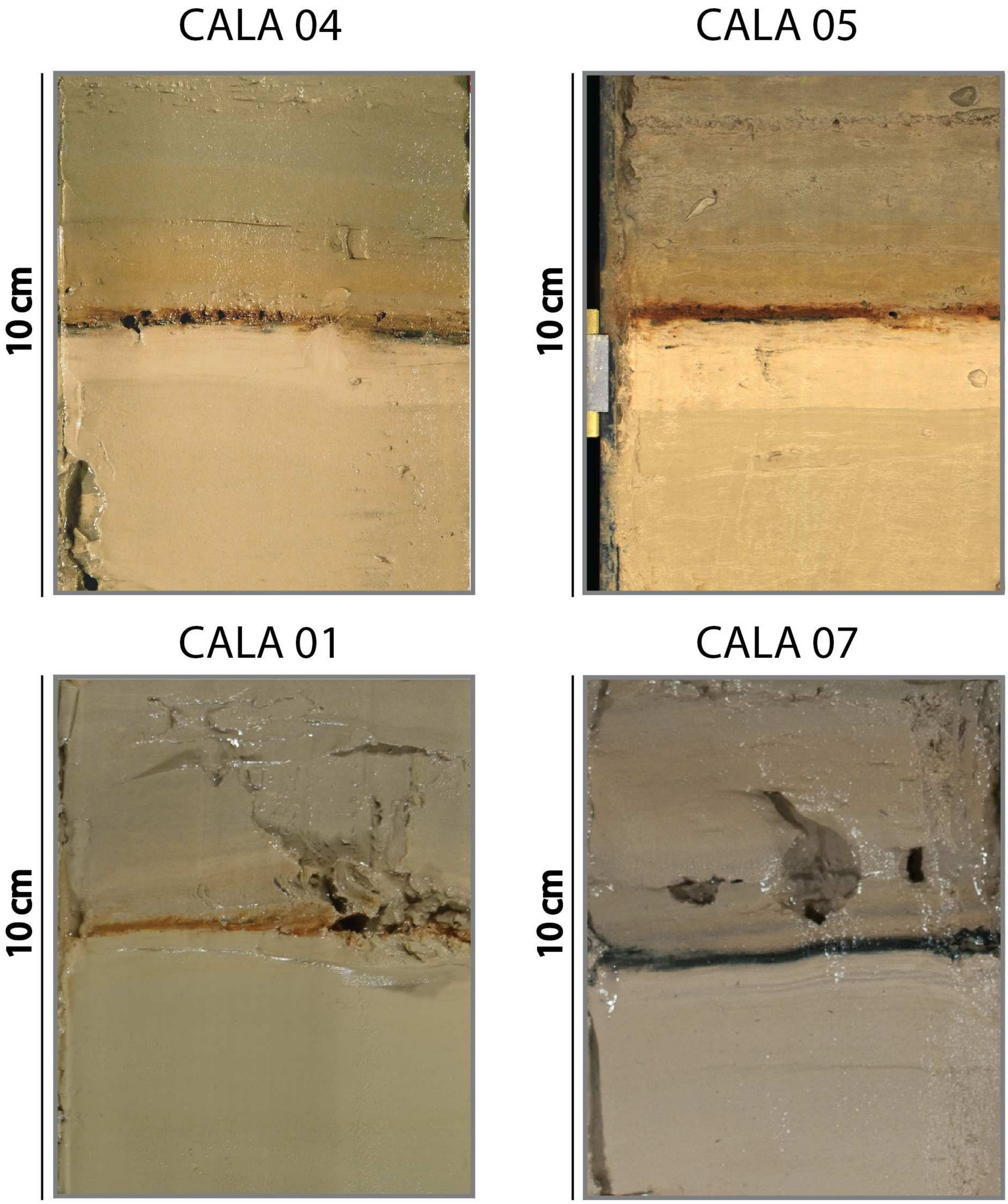

DR3 - A millimetric black and reddish horizon is present at the top of the HAT and is shown for cores CALA 01, 04, 05 and 07). This horizon is enriched in Fe and Mn and shows abundant Fe/Mn micro-nodules. This horizon could represent a diagenetic red-ox front marking the top of the turbidite, caused by mobilization of Fe and Mn within the turbidite following the development of reducing condition induced by the rapid sediment accumulation. The fine-grained upper part of the HAT has an increased concentration of organic carbon whose bacterial oxidation (Polonia et al., 2013a) may lead to reduction of Fe and Mn oxides.

Data repository DR4

Micropalaeontological analyses were performed on 114 samples, integrating previously published data from CALA 04 and CALA 05 (Polonia et al., 2013a). All samples, of 0,5-1,5 cm thick and about 3-8 gr of dried sediments, were dried at 40 °C for 24 h, weighted, soaked in water, wet sieved through sieves of 63 µm, dried and weighted again. Selected samples were dry sieved through sieves of 125, 250 and 500 µm.

The identification of foraminifera was supported by original descriptions and selected key papers such as Banner and Blow (1960), Cita et al. (1974), AGIP (1982), Kennett and Srinivasan (1983) and Rasmussen (2005).

Microfossil assemblage within the **HAT (Fig. DR 1A)**:

Low amount of small planktonic foraminifera (63-125 µm) such as *Tuborotalita quinqueloba* (Natland, 1938) and juvenile specimens of *Globigerinoides ruber* (d'Orbigny, 1839), *Globorotalia scitula* (Brady, 1882), *Globigerinoides* sp., *Globigerina* sp., and *Neogloboquadrina* sp. in association with few pteropod fragments. Samples barren in foraminifera were locally observed.

Microfossil assemblage of pelagic sediments above the HAT **top (Fig. DR 1B)**:

This assemblage consists mainly of abundant planktonic foraminifera, with no evidences of size-selection. Planktonic foraminifera mainly belong to *Globigerinoides ruber Globigerinoides quadrilobatus* (d'Orbigny, 1846), *Globigerinoides sacculifer* (Brady, 1877), *Orbulina universa* (d'Orbigny, 1839), *Globorotalia inflata* (d'Orbigny, 1839), *Globorotalia scitula*, *Globorotalia truncatulinoides excelsa* (Sprovieri, Ruggieri and Unti, 1980), *Globigerinella calida* (Parker, 1962), and *Globigerinella siphonifera* (d'Orbigny, 1839). A few specimens of benthic foraminifera, almost exclusively abyssal taxon *Articulina tubulosa* (Seguenza, 1862) and rare fragments of undefined agglutinated species are observed in association with common fragments of thin-walled pteropods, possibly broken during core recovering or sample treatment.

Microfossil assemblage within **recent turbidite beds (Fig. DR 1C)**:

For these recent turbidites, fossil assemblages are substantially comparable with those of the upper part of the HAT, although an higher amount of size-selected planktonic foraminifera was commonly observed and these are locally (mainly in core CALA 04) associated with few small-sized (< 125 µm) benthic species, such as *A. tubulosa*, *Bolivina dilatata* Reuss, 1850, *Gyroidina* sp., *Cassidulina laevigata* d'Orbigny, 1826 and *Nonion* sp..

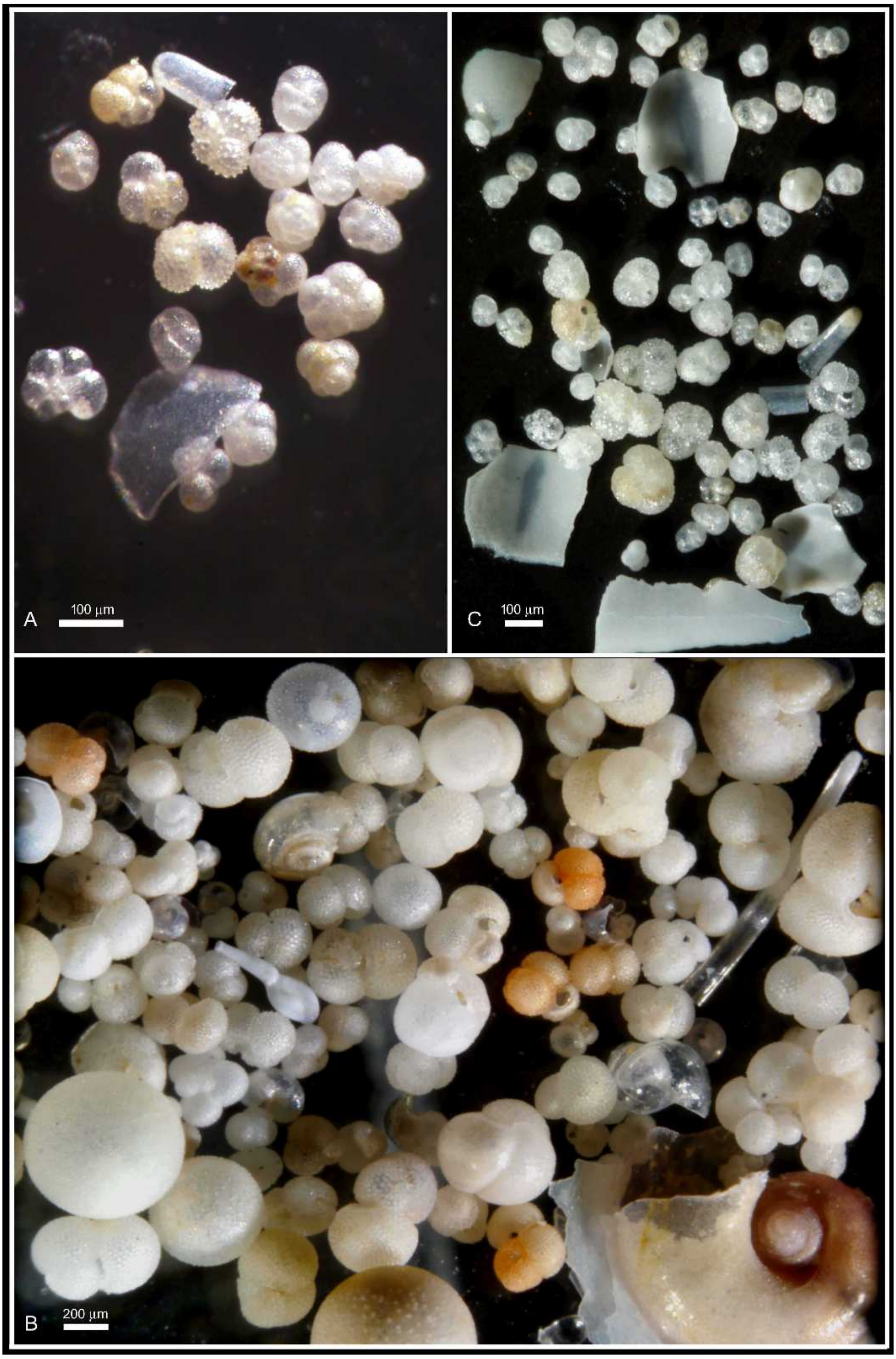

DR4 - Microphotograph of foraminiferal assemblages and pteropod fragments from CALA 07. A: All foraminifera and pteropod fragments from the sample below the HAT top (CALA 07 V, cm 34-35); B: Selected foraminifera and pteropod fragments from the dated pelagic sample above the HAT (CALA 07 V, cm 28-29); C: All foraminifera and selected pteropod fragments from recent turbidite beds (CALA 07 V, cm 23.5-24.5). See X in Figure 2 for sample position in core CALA 07.

Data repository DR5

Accelerator mass spectrometry (AMS) radiocarbon dating was performed on mixed planktonic foraminifera (11 samples) and pteropod fragments (2 samples). Approximately 40-70 mg of pristine planktonic foraminifera or perfectly cleaned pteropod fragments, with no evidence of abrasion or carbonate overgrowth were handpicked in the size fraction > 250 μm in the first available pelagic sample above the HAT including sufficient material for radiocarbon dating.

1 Sample name and depth	2 Core depth (cm)	3 Position relative to the turbidite And type of sample	4 LAT	5 LON	6 Measured 14C age BP	7 Calibrated Age (2 σ) with ΔR=147±43 (weighted mean including 2 ΔR in the surrounding regions)	8 **HAT emplacement time with ΔR=147±43:** dates interpolated on the top of the turbidite
CALA 04	V 8-9	3 cm above the HAT top. Foram	35 39.643	16 34.845	**1860 +/- 30**	AD 578-786	**AD 189-530**
CALA 05	V 49-50	2 cm above the HAT top. Foram	35 42.557	16 40.124	1890 +/- 35	**AD 547-774**	**AD 215-547**
CALA 01	V 19-19,5	Just above the HAT top. Pteropods	36 14.044	17 46.270	2070 +/- 30	**AD 352-609**	**AD 352-609**
CALA 02	V 1-2	1 cm above the HAT top Foram	36 09.848	17 51.760	1629 +/- 29	**AD 789-1028**	**AD 633-964**
CALA 03 (tot m)	VI 3-4	2 cm above the HAT top. Foram	36 05.120	17 57.849	1670 ± 28	**AD 744-998**	**AD 432-870**
CALA 07 (tot m)	V 28-29	1 cm above the HAT top. Foram	35 45.159	16 45.834	1957 ± 27	**AD 464-686**	**AD 308-622**
CALA 08 (tot m)	V 6-7	2 cm above the HAT top. Foram	36 05.776	17 23.991	1792 ± 28	**AD 655-874**	**AD 343-746**
CALA 08 (tot m)	V 6-7	2 cm above the HAT top. Pteropod	36 05.776	17 23.991	1771 ± 28	**AD 669- 889**	**AD 357-761**
CALA 09 (tot m)	VI 34.5-35.5	3 cm above the HAT top. Foram	35 57.991	18 06.990	1644 ± 27	**AD 780-1021**	**AD 222-739**
CALA 09 (tot m)	VI 34.5-35.5	3 cm above the HAT top. Pteropod	35 57.991	18 06.990	1836 ± 29	**AD 602-816**	**AD 44-534**
CALA 10 (tot m)	IV 9.5-10.5	2 cm above the HAT top. Foram	37 36.927	17 43.511	1670 ± 35	**AD 736-1002**	**364-814**

Table DR5 - ^{14}C ages (Poznań Radiocarbon Laboratory - Foundation of the Adam Mickiewicz University, Poland) for CALA samples analyzed in this study. Measured ages were calibrated according to the radiocarbon calibration program *CALIB REV6.0.0* (Stuiver and Reimer, 1993; Stuiver et al., 2005) and results are reported for ΔR=147±43 (column 7) calculated as the weighted mean including 2 ΔR values from published reservoir ages in the surrounding areas (Calib database at http://calib.qub.ac.uk/marine/). The age of the HAT (column 8) was obtained considering the time span corresponding to the thickness of pelagic deposits between the top of the HAT and the dated level.

Data repository DR6

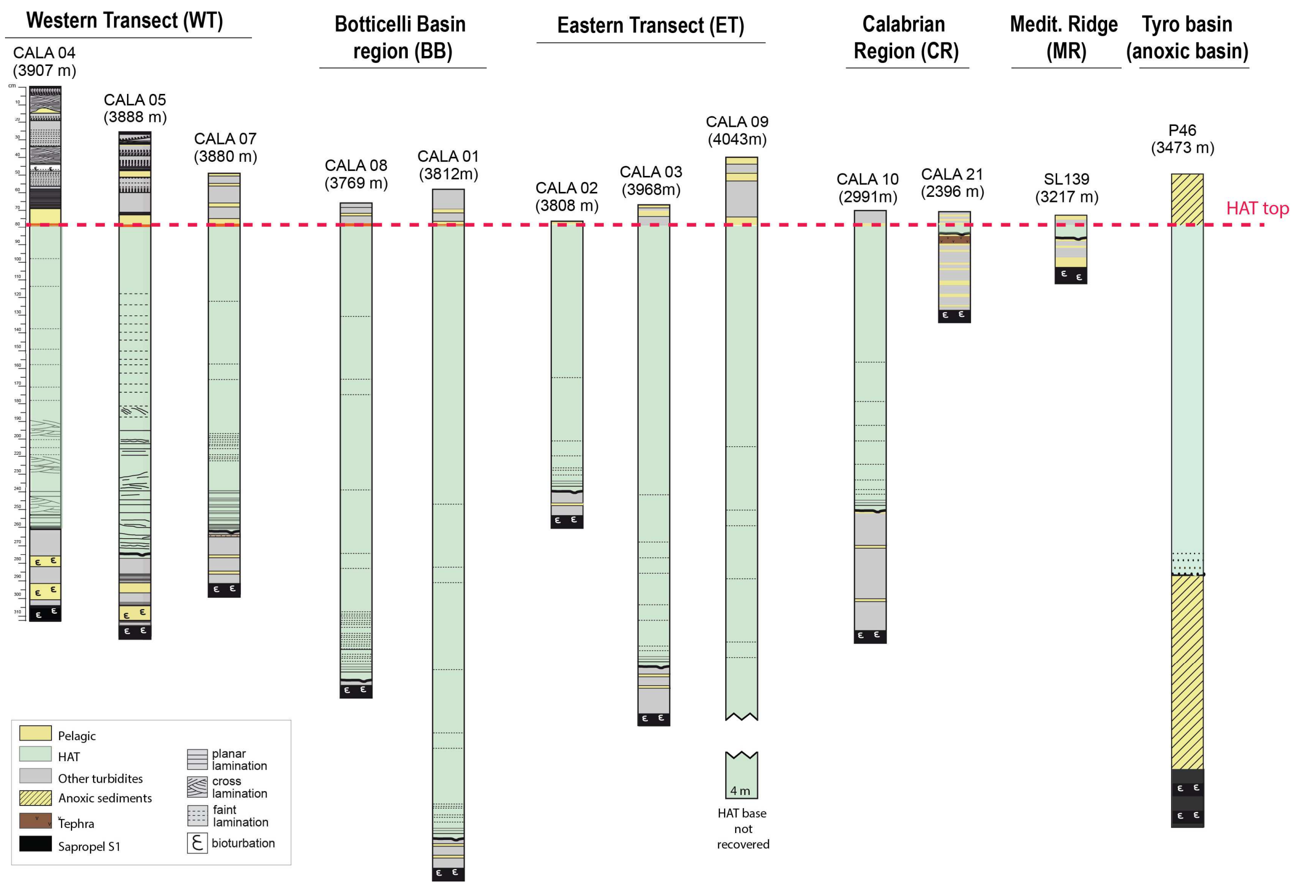

DR6: Stratigraphic log of the analysed cores collected in different physiographic settings: i) abyssal plain at about 4000 m water depth (cores CALA 04 and 09); ii) perched basins on the slopes of the accretionary wedge (cores CALA 05, 07, 08, 01, 02, 03); iii) slopes basins in the inner accretionary wedge (core CALA 10); iv) structural high at about 2400 m water depth (core CALA 21); v) Mediterranean Ridge area (core SL139) and vi) anoxic Tyro basin (core P46). Core locations are represented by red dots in Figure 1. HAT thickness varies between 20 cm (core CALA 21) to more than 12 m in core CALA 09 where the HAT base was not recovered. The basal part of the HAT deposit shows cross and parallel laminations while in the upper part only faint laminations are present. Cores CALA 04 and 05 are described by Polonia et al. (2013a).

Data repository DR 7 **CORE SL139 – MEDITERRANEAN RIDGE AREA**

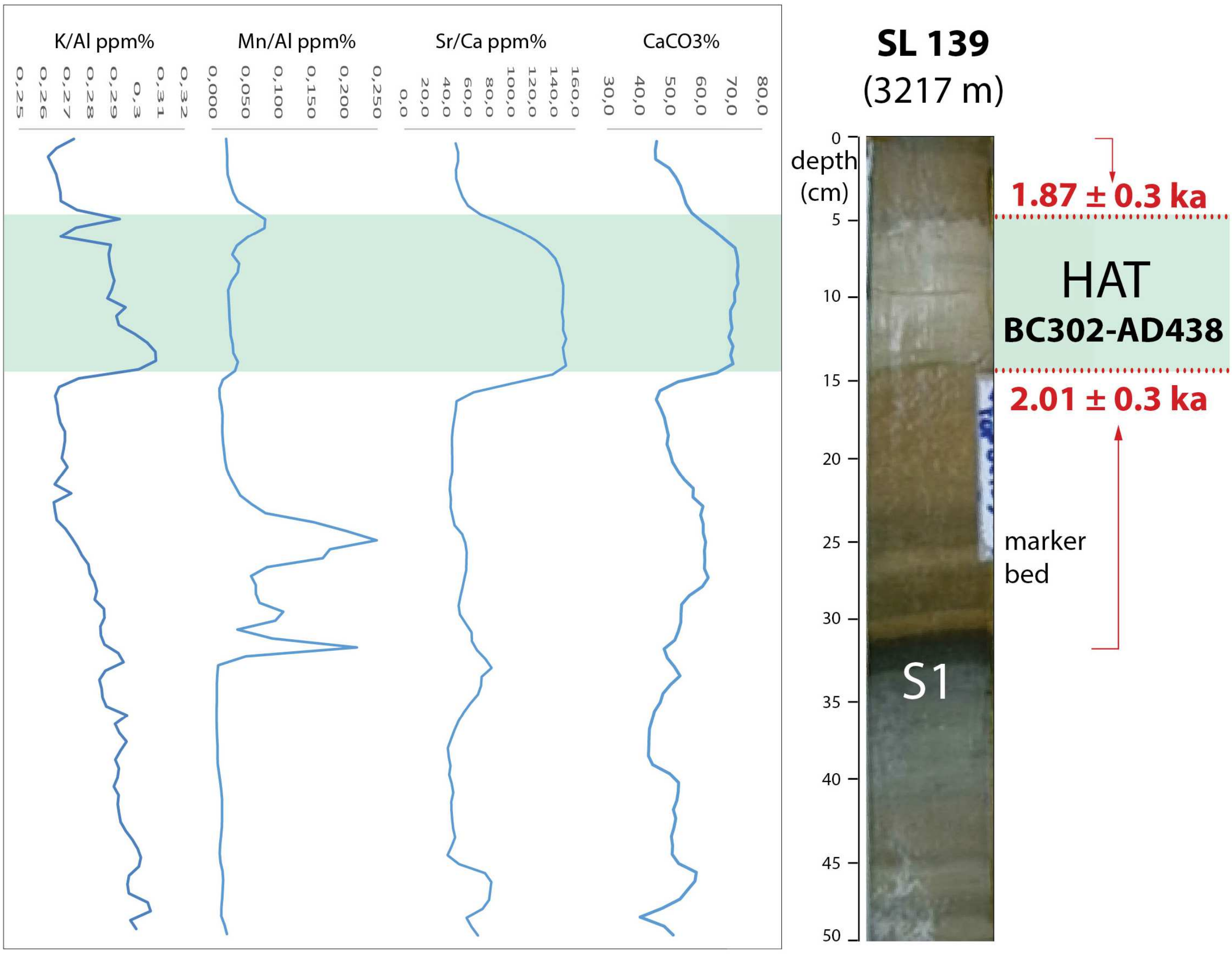

DR7 - In the MR area, ages in core SL139 (34N16.051’; 19E49.794’) were estimated using cal ^{14}C BP ages for top and bottom of S1 (6.1 and 10.8 ka cal BP; De Lange et al., 2008) and 0 ka cal BP for the core top. Extrapolation from top down and from bottom up towards the distinctly present HAT, resulted in estimated age of deposition to be respectively: 1.87 and 2.01 ka cal BP with a stdev of ~0.3 ka. This represents a HAT emplacement time window of 302 BC – 438 AD.

This reconstruction is based on the fact that a large number of cores from the eastern Mediterranean Sea have a constant sedimentation rate throughout (De Lange et al., 2008 Nature Geoscience). For only 2 nearcoastal cores that are thought to be under direct influence of a river system, different sedimentation rates during/post S1 were found (Hennekam et al., 2014 paleoceanography). Thus for our deep-core setting no deviation in sedimentation rate is expected.

Extrapolation of the S1 ages to sed-surface results in ~330 yr (uncal), which is close to what can be expected.

On the basis of these observations, absolute ages can be confidently assigned to S1 boundaries in this setting. Consequently, turbidite deposition age estimated in this way, may have a max deviation of ~300 yr.

The HAT turbidite in core SL 139 is unique throughout the core as evidenced by its sedimentological and geochemical characters. The turbidite bed is characterized by high elemental concentrations of K, Sr and Ca similarly to the HAT turbidite in cores CALA 05 (DR1). Moreover, at its top it shows a peak in Mn which is interpreted to represent a diagenetic red-ox front caused by mobilization of Fe and Mn within the turbidite following the development of reducing condition induced by the rapid sediment accumulation. This Mn-rich layer is present in all other cores and is common only for the HAT turbidite (Supplementary DR2). Other turbidite beds do not show such geochemical anomaly.

Data repository DR8 **CORE P46 – TYRO BASIN**

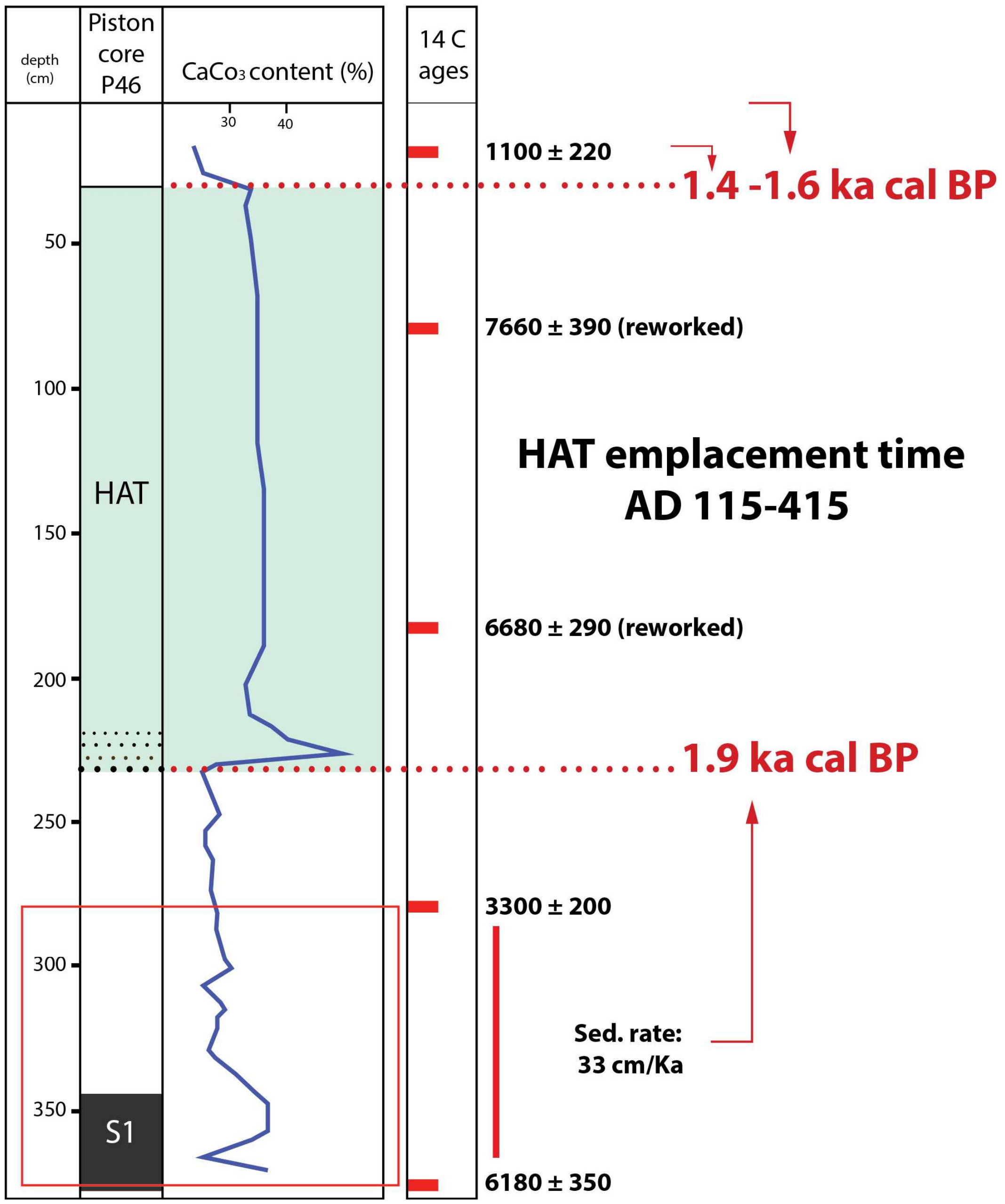

DR8 - Sediment column and ^{14}C dating of core P46 taken within Tyro basin (33°52.54N, 26°02.30E), south of Crete (after Troelstra et al., 1987).

Extrapolating from the lowermost 2 dating points (or using the sedimentation rate (SR) derived from these 2 points: 33 cm/ka) towards the distinct base of the observed HAT at approximately 230 cm, results in an estimated age of deposition of **1.9 ka cal BP.**

Extrapolating from the topmost dating point towards the less distinct top of HAT while using the same SR, results in an age of 1.4 ka cal BP, whereas extrapolating from top of core, assumed to be 0 ka cal BP to 1.1 ka cal BP at ~18cm (or SR=16.4cm/ka), results in an estimated HAT deposition age of: **1.6 ka cal BP.**

These estimates are well within the range for deposition-age of HAT, i.e. related to AD 365 Crete earthquake, but not for that of the Santorini eruption (3.3 ka cal BP).

For core P49, despite the perfect timing we cannot exclude the possibility that a different turbidite was deposited in exactly the same time window because the coring site is very far from other cores. However, another triggering event is unlikely because of these independent observations:

a) The described turbidite in the Tyro basin (from 30 cm to 230 cm in core P46) is 2 m thick. This unit thickness is unique throughout the core as evidenced by the $CaCo_3$ content, which is high only within this turbidite bed, implying that this is an exceptional event occurred after sapropel S1 deposition, related to sedimentary processes capable to resuspend material in a very confined basin isolated from all canyon systems. A tsunami wave is thus the most likely triggering mechanism as suggested for cores CALA 04 and 05 in Polonia et al. (2013a).

b) Five ^{14}C ages are available throughout core P46. Turbidite emplacement age deduced through sedimentation rate estimated using ^{14}C ages is in perfect agreement with results from other cores and centered on the AD 365 earthquake. This is confirmed also by age modeling (DR9).

c) The catalogue of historical earthquakes and tsunamis in the eastern Mediterranean shows only one tsunamigenic earthquake in the time window AD 115-415. This seismic event is the AD 365 Crete earthquake. There are other 4 moderate to large earthquakes (M between 6 and 7.8) in the same time window (Salamon et al., 2008), but they are not associated with tsunamis. Moreover, they occurred in Syria, Lebanon or in Israel (from the Hula Valley to the Dead Sea) hundreds of Km far from the Tyro basin and thus not capable of triggering a 2-m thick turbidite in as isolated basin south of Crete not fed by canyon systems.

Data repository DR9

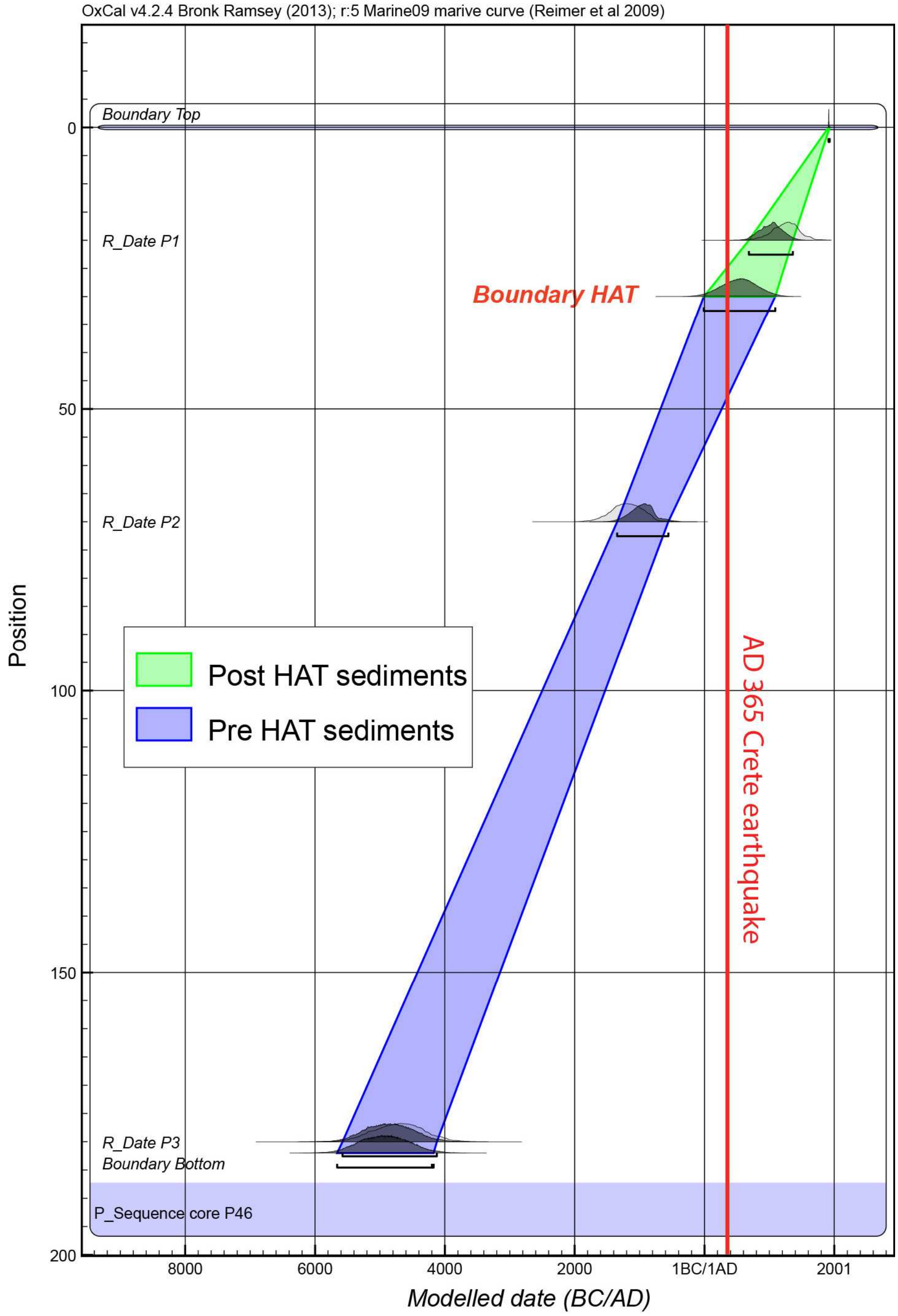

DR9 – Age modeling for core P46 in the Tyro basin (Troelstra et al., 1987). We have built a depositional model with the OxCal software[30] from the order of deposition of pelagic sediments and their depth derived subtracting the thickness of the HAT turbidite from the total core. The software identifies mathematically a set of possible ages for each depth point in the sedimentary sequence; age distributions at 2σ are modelled from their stratigraphic depth of emplacement into the background sequence. Despite uncertainties intimately related to this method, age modelling allowed us to deduce the following main conclusions: 1) sedimentation rate is constant throughout the core in agreement with our assumptions; 2) the HAT age distribution is centred on the AD 365 Cretan earthquake (red line). This implies that the described turbidite in the Eastern Mediterranean may represent the same catastrophic event as in the Ionian Sea.

References:

AGIP, 1982, Foraminiferi Padani (Terziario e Quaternario): Milan, Italy, AGIP, Plate I—LII.

Banner, F.T., and Blow, W.H., 1960, Some primary types of species belonging to the superfamily Globigerinaceae: Contributions from the Cushman Foundation for Foraminiferal Research, v. 11, no. 1, p. 1–41.

Bronk Ramsey, C., and Lee, S., 2013, Recent and Planned Developments of the Program OxCal. Radiocarbon, v. 55, p. 720-730.

Cita, M.B., Ciampo, G., Ferone, E., Moncharmont Zei, M., Scorziello, R., and Taddei Ruggiero, E., 1974, Il Quaternario del Tirreno abissale. Interpretazione stratigrafica e paleoclimatica del pozzo DSDP 132: Revista Española de Micropaleontologia, v. 2, p. 257-326.

De Lange, G.J., Thomson, J., Reitz, A., Slomp, C.P., Principato, M.S., Erba, E., and Corselli, C., 2008, Synchronous basin-wide formation and redox-controlled preservation of a Mediterranean sapropel: Nature Geoscience, v. 1, p. 606-610.

Gasperini, L., and Stanghellini, G, 2009, SeisPrho: An interactive computer program for processing and interpretation of high-resolution seismic reflection profiles: Computers & Geosciences, v. 35, no. 7, p. 1497–1507.

Hennekam, R., T. Jilbert, B. Schnetger, and G. J. de Lange (2014), Solar forcing of Nile discharge and sapropel S1 formation in the early to middle Holocene eastern Mediterranean, Paleoceanography, 29, 343–356, doi:10.1002/2013PA002553.

Kennett, J.P., and Srinivasan, M.S., 1983, Neogene planktonic foraminifera: a phylogenetic atlas: Stroudsburg, Pennsylvania, Hutchinson Ross Publishing Company, 265 p.

Polonia, A., Bonatti, E., Carmelenghi, A., Lucchi, R.G., Panieri, G., and Gasperini, L., 2013a, Mediterranean megaturbidite triggered by the AD 365 Crete earthquake and tsunami: Scientific Reports, 3, Article number 1285, doi:10.1038/srep01285.

Polonia, A., Panieri, G., Gasperini, L., Gasparotto, G., Bellucci, L.G., and Torelli, L., 2013b, Turbidite paleoseismology in the Calabrian Arc Subduction Complex (Ionian Sea): Geochemistry, Geophysics, Geosystems, v. 14, no. 1, doi 10.1029/2012GC004402.

Rasmussen, T.L., 2005, Systematic paleontology and ecology of benthic foraminifera from the Plio-Pleistocene Kallithea Bay Section, Rhodes, Greece, *in* Rasmussen, T.L., Hastrup, A, and Thomsen, E., eds., Lagoon to Deep-Water Foraminifera and Ostracods from the Plio-Pleistocene Kallithea Bay Section, Rhodes, Greece: Fredericksburg, Virginia, Cushman Foundation Special Publication, no. 39, p. 53-157.

Reimer, P.J., Baillie, M.G.L., Bard, E., Bayliss, A., Beck, J.W., Blackwell, P.G., Bronk Ramsey, C., Buck, C.E., Burr, G.S., Edwards, R.L., Friedrich, M., Grootes, P.M., Guilderson, T.P., Hajdas, I., Heaton, T.J., Hogg, A.G., Hughen, K.A., Kaiser, K.F., Kromer, B., McCormac, F.G., Manning, S. W., Reimer, R. W., Richards, D.A., Southon, J.R., Talamo, S., Turney, C.S.M., van der Plicht, J., and Weyhenmeyer, C.E., 2009, IntCal09 and Marine09 radiocarbon age calibration curves, 0-50,000 years cal BP: Radiocarbon, v. 51, p. 1111-1150.

Salamon, A., Rockwell, T., Ward, S.N., Guidoboni, E., Comastri, A., 2007, Tsunami hazard evaluation of the eastern Mediterranean: historical analysis and selected modeling: Bulletin of the Seismological Society of America, v. 97, p. 705–724.

Stuiver, M., and Reimer, P., 1993, Extended ^{14}C data base and revised CALIB 3.0 ^{14}C age calibration program: Radiocarbon, v. 35, p. 215–230.

Stuiver, M., Reimer, P.J., and Reimer, R.W., 2005, CALIB 5.0. (WWW program and documentation: http://calib.qub.ac.uk/calib/, access 01/23/2013).

Troelstra, S.R., 1987, Late Quaternary sedimentation in the Tyro and Kretheus basins, Southeast of Crete: Marine Geology, v. 75, p. 77–91.